A Tenuous Carbon Dioxide Atmosphere on Jupiter's Moon Callisto

Robert W. Carlson

Jet Propulsion Laboratory
California Institute of Technology
Mail Stop 183-601
4800 Oak Grove Drive
Pasadena, CA 91109

E-mail: rcarlson@lively.jpl.nasa.gov

Submitted to Science
(Received November 3, 1998)

Abstract

An off-limb scan of Callisto was conducted by the Galileo Near Infrared Mapping Spectrometer to search for a carbon dioxide atmosphere. Airglow in the CO_2 ν_3 band was observed up to 100 km above the surface and indicates the presence of a tenuous carbon dioxide atmosphere with surface pressure of 7.5×10^{-12} bar and a temperature of about 150 K, close to the surface temperature. A lifetime of order 4 years is suggested, based upon photoionization and magnetospheric sweeping. Either the atmosphere is transient and was formed recently, or some process is currently supplying CO_2 to the atmosphere.

Three of the four Galilean satellites of Jupiter are known to possess rarified atmospheres, and their properties are indicative of surface processes and composition. Io's SO_2 atmosphere (1) arises from volcanic emissions and sublimation. Europa (2,3) has an O_2 atmosphere, and molecular oxygen (3) and atomic hydrogen (4) gases have been found on Ganymede. For the latter two moons, radiolysis of surface ice is thought to produce the observed atmosphere (2,3,5). The presence of carbon dioxide (CO_2) in the surface material of the icy Galilean moons was inferred (6,7) using data from the Galileo spacecraft's Near Infrared Mapping Spectrometer (NIMS, 8). If these surface identifications are correct, then the volatility of CO_2 suggests the corresponding presence of CO_2 atmospheres. This hypothesis was investigated for the outermost Galilean satellite, Callisto, by searching for characteristic airglow emissions produced by resonance scattering and fluorescence of solar radiation in the strong ν_3 fundamental stretching band of CO_2 at 4.26 μm.

An off-limb scan was performed by the Galileo spacecraft during a close flyby of Callisto (9). The equatorial noon region vertically above the surface was scanned by NIMS for tangent altitudes $z > 300$ km down to $z = 0$. Spectra were obtained at about 5 km intervals, with the instantaneous vertical resolution ≤ 2 km. The spectral resolution of NIMS is 0.025 μm (full width at half maximum, FWHM) and a fast (4 1/3 sec) spectral scan mode provided spectral measurements at 0.025 μm increments. The CO_2 ν_3 band consists effectively of ~ 40 P and R-branch rotational lines in the 4.2 to 4.3 μm region (mean spacing ~ 0.003 μm, Doppler width ~ 3×10^{-6} μm at 150 K), The line structure is unresolved at the modest resolution of NIMS and only the band envelope is obtained.

Signal enhancement above the dark level is evident for wavelengths within the CO_2 band (Fig. 1B) in the ~100 km region above the surface. Spectral channels outside the band (Fig. 1A, C) show no such enhancement; therefore the in-band signal is not due to instrumental stray light from the nearby bright limb. The emission data (Fig. 1B) are compared with a theoretical altitude profile (described later) and found to be consistent with an atmosphere at a temperature of $T = 150 \pm 50$ K.

The spectral profile of the emission feature, obtained by averaging spectra from the lowest 40 km, is shown in Fig. 2 along with a theoretical band profile. The measured feature agrees with expectation in position and width. These spectral agreements, together with the consistent vertical profile, provide evidence that Callisto possesses a tenuous atmosphere of carbon dioxide.

The atmospheric abundance of CO_2 was determined using radiative transfer theory for the scattering of resonance radiation by atoms and molecules. The complete–frequency-redistribution approximation (10) was used, which assumes that the molecules absorb and emit with a Doppler (Gaussian) profile. The theory was generalized for the present case of coupled P- and R-branch vibration-rotation lines. Isotropic scattering was used to compute source functions for singly and multiply scattered light. Anisotropic scattering was incorporated using the phase function from Placzek (11) to modify the isotropic single-scattering source function (12) and to correct the amplitude of the multiply scattered radiation (13). The derived source functions were then used with spherical geometry to compute limb brightness profiles and band shapes. Absorption cross sections were obtained from the HITRAN 96 compilation (14); Hönl-London factors (15) were used for the line branching ratios.

Computed intensities and profiles are compared with the observations in Fig. 1B and Fig. 2. These curves were computed for an isothermal atmosphere at $T = 150$ K and a surface pressure of $p(0) = 7.5$ pbar. The derived temperature is close to the noon surface temperature of Callisto (16) and the corresponding scale height of the assumed exponential atmosphere is $H = 23$ km. The number density at the surface is $n(0) \approx 4\times10^{8}$ cm^{-3} and the vertical column abundance is $N = n(0)\,H \approx 8\times10^{14}$ cm^{-2}, with possible errors of approximately ± 60 %. At this low CO_2 abundance, and in the absence of other gases, the atmosphere would be nearly collisionless, constituting an exosphere. However, other gases may be present (e.g. H_2O and the photochemical products of CO_2 – carbon monoxide and oxygen).

The vertical optical depths at the centers of the Doppler-broadened lines are $\lesssim 1$, so the net atmospheric absorption is less than 0.5% and smaller than the observed surface-related absorption (6,7). There is about one hundred times more CO_2 in the optically-sensed surface layer (~ 100 μm thick) compared to the overlying column of gas, and the surface component must be only loosely coupled to the atmosphere because the surface CO_2 concentration correlates with presumably ancient morphological features (7). This long-lived surface CO_2 may be trapped in bubbles (7, 17), occur in mineral fluid inclusions (7), or perhaps be sorbed in zeolitic silicates. There will also be a more mobile surface component, formed by the momentary sticking of atmospheric molecules that impinge on the surface. It is expected to be small compared to the immobile component and to exist as a temperature-dependent partial layer of monolayer dimensions.

It is not possible to determine the extent of the atmosphere from this single observation, but the mobility and volatility of CO_2 suggests a global atmosphere. The surface pressure (7.5 pbar) corresponds to the vapor pressure of CO_2 ice at 75 K (18), prompting speculation that the atmosphere may be buffered by deposits of CO_2 ice in cold, permanently shadowed regions. While this is plausible, there are other mechanisms that can influence the CO_2 concentration. The concentration of CO_2 in water ice and the sublimation rate of H_2O may limit effusion of CO_2 from the surface. However, water molecules probably segregate into localized cold traps of high albedo frost (19). Carbon dioxide, being much more volatile, may follow a different thermal segregation, becoming independent of water sublimation rates.

Another influence on the CO_2 abundance is loss induced by ultraviolet radiation. The diurnally averaged photoionization rate (20) is 1.5×10^{-8} sec^{-1} and the photoions can be rapidly swept away by the co-rotating jovian magnetic field. If half of the ions are lost and there is no replenishment, the lifetime τ of a CO_2 atmosphere would be only 4 years. Unless the sweeping efficiency is grossly overestimated, or if there is shielding provided by some other ultraviolet absorber, then a relatively short life is expected. Either this atmosphere is recent and transient, or some supply mechanism is currently operating on Callisto. For steady state, a source of $\varphi = N/\tau = 6\times10^6$ molecules cm^{-2} sec^{-1} is required, using the above loss rates. Electron ionization and photodissociation may increase the loss rate and the corresponding source flux.

There are numerous possibilities for CO_2 sources, including outgassing from the interior. Indeed, evidence for sublimational erosion of Callisto's surface by CO_2 has been found by Moore et al.'s (21) analysis of Galileo images. The original source of this internal CO_2 could be direct accretion, during formation, of material containing CO_2, or by subsequent internal aqueous-alteration of primitive carbonaceous compounds (22).

Alternatively, the atmospheric and surficial CO_2 may involve only the surface, not the interior. Ultraviolet and charged particle interactions could produce and release CO_2 from endogenic or exogenic carbon-bearing surface material (5, 23). Chemical production of CO_2 and other volatiles can occur in large impacts (24), and perhaps during more frequent micrometeoritic bombardment. Another source could be the direct accretion of CO_2 from cometary material. The recent observation of carbon dioxide in the stratospheres of Jupiter, Saturn, and Neptune (25) may help to resolve this question because the existence of CO_2 above the tropopause cold traps might require external sources.

REFERENCES AND NOTES

1. E. Lellouch, *Icarus* **124**, 1 (1996).

2. D. T. Hall, D. F. Strobel, P. D. Feldman, M. A. McGrath, H. A. Weaver, *Nature* **373**, 677 (1995).

3. D. T. Hall, P. D. Feldman, M. A. McGrath, D. F. Strobel, *Astrophys. J.* **499**, 475 (1998).

4. C. A. Barth et al., *Geophys. Res. Lett.* **24**, 2147 (1997).

5. R. E. Johnson, R. M. Killen, J. H. Waite, Jr., W. S. Lewis, *Geophys. Res. Lett.* **25**, 3257 (1998).

6. R. Carlson et al., *Science* **274**, 385 (1996); T. B. McCord et al., *Science* **278**, 271 (1997); W.D. Smythe et al., paper presented at the XXIX Lunar and Planetary Science Conference, Houston, Texas 16-20 March 1998.

7. T. B. McCord et al., *J. Geophys. Res.* **103**, 8603 (1998). The surface-related CO_2 is ubiquitous on Callisto and exhibits spatial variations that correlate with morphological features.

8. R. W. Carlson, P. R. Weissman, W. D. Smythe, J. C. Mahoney, the NIMS Science and Engineering Teams, *Space. Sci. Rev.* **60**, 457 (1992).

9. The atmospheric was scanned above the Callisto's limb during the tenth orbit (C10) of Galileo around Jupiter, immediately following a close flyby of Callisto (17 Sept. 1997 at 00:21 UT). Callisto was at 75° orbital phase and the observation scanned tangentially through the atmosphere above the region at 80° - 90° W, 2° N. The range to Callisto varied from 2100 km to 3800 km over the ~6 minute spatial scan. A total of 65 spectra were obtained for tangent altitudes ranging from zero to 300 km above the surface. Each spectrum has 24 wavelength channels, 12 for CO_2 detection and 12 for H_2O detection.

10. T. Holstein, Phys. *Rev.* **72**, 1212 (1947); T. M. Donahue and R. R. Meier, *J. Geophys. Res.* **72**, 2803 (1967); T. Tohmatsu and T. Ogawa, *Rep. Ionosph. Space Res. Japan* **20**, 418 (1966).

11. G. Placzek, in *Handbuch der Radiologie*, E. Mars, Ed. (Akademische Verlagsgesellschaft VI, Leipzig, 1934) Vol. 2, pp. 209-374, Chapters 6 and 25.

12. This approximation assumes that most of the effect of anisotropic scattering occurs in the primary scattering and that successive multiple scattering loses memory of the incident direction and can be treated as isotropic. R. W. Carlson and D. L. Judge, in *Jupiter*, T. Gehrels, Ed. (Univ. Arizona Press, Tucson, 1976), p. 433; B. Hapke, *J. Geophys. Res.* **86**, 3039 (1981).

13. The source functions for multiply scattered light were initially computed using the assumption of isotropic scattering. However, the amount of energy reabsorbed in the medium after the primary scattering, and then available for multiple scattering, depends upon the initial scattering pattern. It is different for the assumed isotropic scattering case and the anisotropic scattering pattern of CO_2 molecules. A correction is therefore applied to the multiply scattered source function to account for this effect.

14. L. S. Rothman et al., *J. Quant. Spectrosc. Radiative Trans.*, in press.

15. G. Herzberg, in *Molecular Spectra and Molecular Structure, II: Infrared and Raman Spectra of Polyatomic Molecules* (Van Nostrand, Princeton, 1945) p. 422.

16. R. Hanel et al., *Science* **206**, 952 (1979); J. R. Spencer, thesis, University of Arizona (1987).

17. R. E. Johnson and W. A. Jesser, *Astrophys. J.* **480**, L79 (1997).

18. S. Dushman and J. M. Lafferty, *Scientific Foundations of Vacuum Technique* (Wiley, New York, 1962), pp. 726-728.

19. J.R. Spencer, *Icarus* **69**, 297 (1987).

20. W. F. Huebner, J. J. Keady, S. P. Lyon, *Astrophys. Space Sci.* **195**, 1 (1992).

21. J. M. Moore et al., *Icarus*, submitted.

22. E. L. Shock and W. B. McKinnon, *Icarus* **106**, 464 (1993).

23. M. L. Delitsky and A. L. Lane, *J. Geophys. Res.* **102**, 16385 (1997).

24. K. Zahnle, J. B. Pollack, D. Grinspoon, L. Dones, *Icarus* **95**, 1 (1992).

25. T. deGraauw et al., *Astron. Astrophys.* **321**, L13 (1997); H. Feuchtgruber et al., *Nature* **389**, 159 (1997); T. Encrenaz, paper presented at The Jovian System after Galileo, The Saturnian System before Cassini-Huygens Conference, Nantes, France 11-15 May 1998; E. Lellouch et al., *ibid.*

26. I thank Marcia Segura for implementing the observing sequence, Bob Mehlman for data processing, and Fraser Fanale for pointing out the possibility of water sublimation limiting CO_2 effusion. The work described herein was performed at the Jet Propulsion Laboratory, California Institute of Technology, under contract with the National Aeronautics and Space Administration.

FIGURE CAPTIONS

Fig. 1. Vertical brightness profiles inside and outside the ν_3 band. (A) and (C) are for 0.025 μm wide (FWHM) wavelength channels outside the CO_2 ν_3 band [4.07 μm for (A), 4.36 μm for (C)]. No signal is evident. The data in (B) are for a wavelength interval containing the entire CO_2 band (effective range 4.20 to 4.31 μm). This profile indicates atmospheric airglow emission emanating from the 100-km region above the surface. A theoretical vertical profile for the total band intensity is also shown for the nominal case: $p(0) = 7.5$ pbar, $T = 150$ K. One kR (1000 Rayleighs) is a column emission rate of 10^9 photons sec^{-1}. The data in (B) are the sum of five spectral channels, and therefore noisier by the factor $\sqrt{5}$ than the single-channel measurements of (A) and (C).

Fig. 2. Observed and predicted band shape. Spectra obtained for tangent altitudes from 5 to 40 km were combined to form the average spectrum shown as points. The curve is for theoretical spectra averaged over the same altitude interval and convolved to NIMS resolution. Nominal conditions of $p(0) = 7.5$ pbar and $T = 150$ K were used to generate the theoretical profile. The position and width of the observed feature indicates that CO_2 ν_3 band atmospheric emissions were observed.

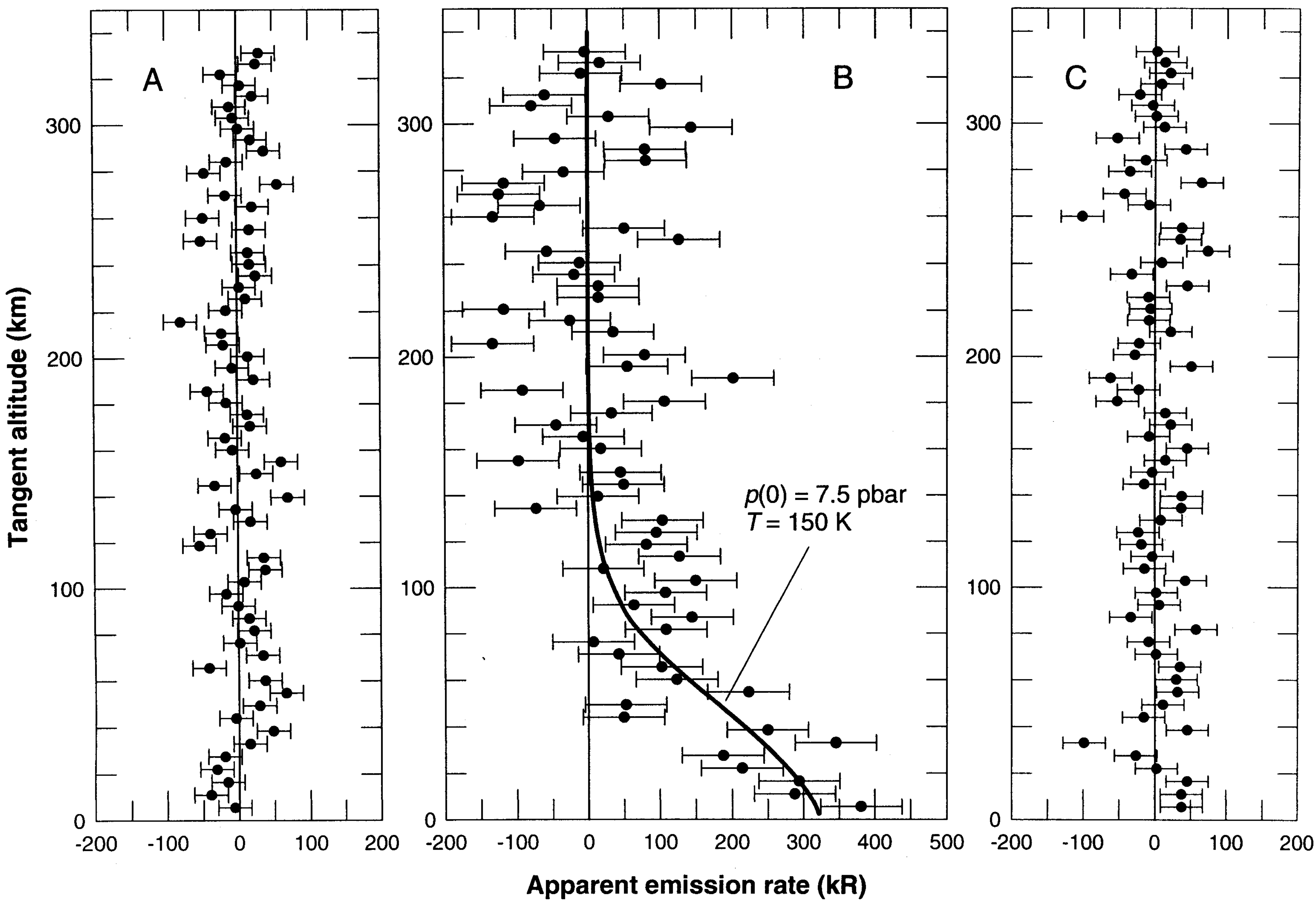

A
B
C
Tangent altitude (km)
Apparent emission rate (kR)
$p(0)$ = 7.5 pbar
T = 150 K

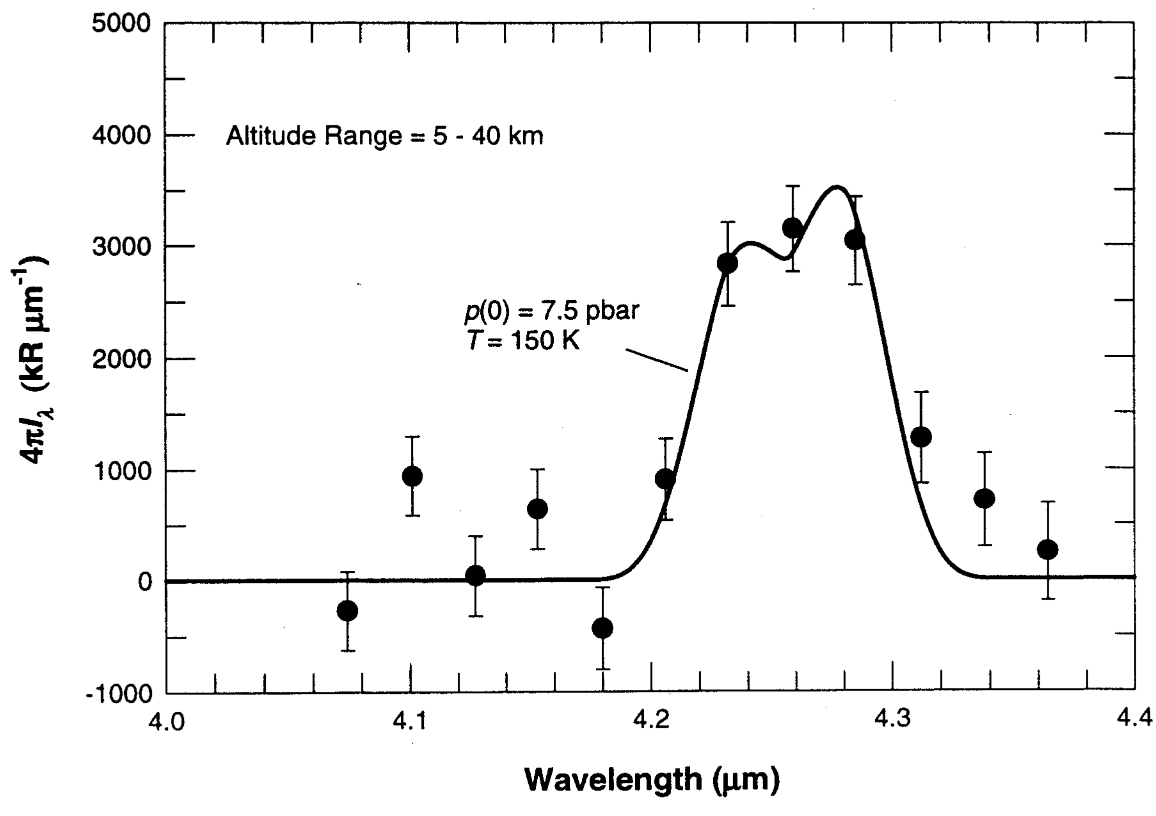

Altitude Range = 5 - 40 km
p(0) = 7.5 pbar
T = 150 K
4πI_λ (kR μm^-1)
Wavelength (μm)
5000
4000
3000
2000
1000
0
-1000
4.0
4.1
4.2
4.3
4.4